

Power Number Calculations for a Taylor-Couette Flow

R.SRINIVASAN, S.JAYANTI*, A.KANNAN

Department of Chemical Engineering
Indian Institute of Technology Madras
Chennai 600036

INDIA

sjayanti@iitm.ac.in <http://www.che.iitm.ac.in/~sjayanti/>

Abstract: The classical problem of Taylor-Couette flow between rotating concentric cylinders under laminar flow conditions is studied using computational fluid dynamics (CFD) techniques. The flow between concentric cylinders with the inner cylinder rotating and the outer cylinder stationary for a Newtonian fluid has been calculated for a range of Reynolds numbers, radius ratios, length to diameter ratios using the CFD code *CFX*. The predicted tangential velocity profiles have been found to agree well with analytical profiles in the Couette flow regime and the transition from Couette flow to Taylor vortex flow has also been correctly predicted. Results for the power number show that it varies inversely with Reynolds number in the Couette flow regime and as Re^{-n} where $n \sim 0.7$ in the Taylor vortex flow. These results agree well with the experimental data of Sinevic et al [1]. A new correlation is proposed to calculate the power number for the Couette flow and the Taylor vortex flow regimes.

Key-Words: - Rotating cylinders, Computational fluid dynamics, Taylor vortices, Power number, Couette flow, Laminar Taylor vortex flow.

1 Introduction

Taylor-Couette flow is a classical problem in fluid mechanics, and has been the subject of extensive theoretical and experimental investigations since the early work of Taylor [2] in 1923. The flow situation consists of a pair of concentric cylinders with a fluid-filled gap in between; as the inner cylinder is rotated, a shearing flow (the Couette flow) is established between the cylinders, and this becomes unstable to axisymmetric rolls (Taylor vortices) at a critical value of the rotation rate as measured by a dimensionless Reynolds number [3, 4]. Further increase in the rotational speed of the inner cylinder sees the establishment of several stable vortex patterns over the wide transitional region between laminar Couette flow and turbulent vortex flow [3, 5]. The presence of Taylor vortices increases mixing within the annular region, and therefore has advantages in filtration and polymerization. Taylor vortices exhibit the unique mixing behavior of excellent radial mixing combined with minimal longitudinal mixing. Significant enhancement of the mass transfer coefficient over the Couette flow regime is possible under such cases as has been demonstrated experimentally [6] and theoretically [7, 8]. Many of the earlier studies have been done either for high Reynolds numbers or for small clearances. The clearances used for mass transfer applications are usually much larger and also have a relatively small length to diameter ratio. In the

present paper, we take advantage of the accuracy of computational fluid dynamics (CFD) simulations for laminar flow calculations to study the flow field for a Newtonian flow under these conditions.

2 Problem Formulation

2.1 Governing Equations

The basic equations solved are the conservation of mass and momentum describing the flow of a constant property incompressible Newtonian fluid.

Continuity equation:

$$\nabla \cdot \mathbf{u} = 0 \quad (1)$$

Momentum equation

$$\frac{\partial \mathbf{u}}{\partial t} + (\nabla \cdot \mathbf{u} \mathbf{u}) = -\frac{1}{\rho} \nabla p + \nu \nabla^2 \mathbf{u} \quad (2)$$

Here \mathbf{u} is the velocity vector; p is the static pressure, ρ is the density and ν is the kinematic viscosity. Since the fluid under consideration is a liquid and the velocities are small, a constant-property fluid assumption is made.

2.2 Flow Domain and Boundary Conditions

The flow domain consists of the annular region between an inner rotating cylinder and an outer

stationary cylindrical vessel and is completely filled with a liquid. Both the cylinders are concentric with the axis of the vessel. The problem has been formulated as a steady flow problem in cylindrical coordinates with the wall of the inner cylinder moving away at a given tangential velocity. The axial, radial and tangential components are u , v , and w respectively. A no-slip boundary condition with tangential velocity equal to $\Omega \cdot R_i$, where Ω is the angular velocity of the rotating cylinder, and R_i is the radius of the inner cylinder, is imposed at the inner cylinder while a zero velocity no-slip condition is specified on the surface of the stationary outer cylinder. The top and the bottom surface are set to a shear-free surface and a stationary wall, respectively. Since the major flow is in the circumferential direction, all the three velocity components have to be resolved. For this reason, the flow in a 45° sector the cylinder is simulated and a periodic condition is imposed on the two bounding circumferential planes.

2.3 Numerical solution

The solution of the coupled mass, momentum equations for various cases has been carried out using the commercially available CFX 4.4 computer code developed by AEA Technology, UK. It is a general purpose CFD code which uses a finite volume method for the discretization of the governing partial differential equations on a non-staggered, structured, body-fitted grid. The checkerboard type of oscillations of pressure and velocity that are associated with the use of a non-staggered grid are eliminated using the Rhie-Chow interpolation scheme [9] to estimate the face velocities. The pressure-velocity coupling for incompressible flows is effected using the SIMPLE family of schemes [10] adapted for a non-staggered body-fitted grid. The convection terms in the governing flow equations have been discretized using the third order accurate QUICK scheme [11] while the diffusion terms have been discretized using the second order accurate central scheme. The overall accuracy of the discretization is thus formally second order. Typically, a 100×96 non-uniform grid was used to discretize the two-dimensional flow domain in the x - r (axial-radial) plane. The grid is uniform in the axial direction but is very fine in the radial direction near the inner wall where large velocity gradients are expected to occur. Preliminary calculations were made with different grids to check for grid independence of the results.

The progression of the iterative solution of the coupled set of linearized and discretized governing was monitored in several ways: by examining the

evolution of the field values at a particular point in the flow domain; by looking for significant reduction in the absolute values of the residuals of all the equations; by examining the evolution of the velocity profiles and finally by monitoring the torque on the inner cylinder. It was found that a large number of iterations (typically 10000 to 30000) were required for convergence for low Reynolds numbers.

2.4 Estimation of Power number

The power required for maintaining a steady rotational speed of the inner cylinder is estimated directly from the calculation of the total torque required to rotate the inner cylinder. The torque on the cylinder can be readily calculated as:

$$T = \sum_i (\tau_z)_i A_i R_i \quad (3)$$

where τ_z is the computed z -component of the shear stress on the i^{th} control volume having the inner cylinder as one of the surfaces, A_i is the surface area on which the torque is acting, R_i is the radius of the inner cylinder. The summation is carried over all the cells in the ' i 'th direction. The power required for rotation of the cylinder at steady rotational speed N revolutions per second is then given by:

$$P = 2\pi N T \quad (4)$$

and the power number Po , is computed as

$$Po = \frac{P}{\rho N^3 D_i^5} \quad (5)$$

where ρ is the density of the liquid, D_i is the diameter of the inner cylinder. The above procedure of power estimation reduces the computational time requirement, by eliminating the transient solution of the energy equation to deduce the power from viscous energy dissipation. This approach has previously used by one of the authors [12] to calculate the power number for paddle mixing in unbaffled vessels.

3 Results & Discussion

Calculations in a rotating cylinder have been made for several cases to investigate the effect of height-to-hydraulic diameter (L/D_h) ratio, the ratio of the inner-to-outer cylinder radius ratio (η) and the Reynolds number (based on inner diameter) on the power number. The dimensions used in the present calculations are shown in Table 1. The results from these calculations are discussed below.

Table 1. Dimensions used in present calculations.

	Case A	Case B	Case C
Inner radius R _i (m)	0.015	0.015	0.015
Outer radius R _o (m)	0.02375	0.0325	0.05
Gap width d (m)	0.00875	0.0175	0.035
Radius ratio η	0.632	0.462	0.300
Cylinder height L (m)	0.12	0.12	0.12
L/D _h	6.85	3.42	1.71
Reynolds number Re _D	1 ~ 1000		

3.1 Flow field

The radial profiles of the circumferential velocity at Reynolds number Re_D (based on diameter and the surface speed of the inner cylinder) of 25 (Couette flow) & 500 (Taylor vortex flow) are shown in Figure 1 for a radius ratio of 0.30 at mid-height of the cylinder. The velocity profiles are plotted in dimensionless form in which the circumferential velocity is divided by the surface speed (= Ω*R_i, where R_i is the radius of inner cylinder and Ω is the angular velocity) and the radial distance from the wall of the inner cylinder is divided by the gap width. The radial profile of the tangential velocity component is found to be nearly linear and independent of Reynolds number for low Re_D and a boundary-like flow is developed for high Re_D. It can be seen that under Taylor vortex flow condition, the central, well-mixed region has a small radial gradient.

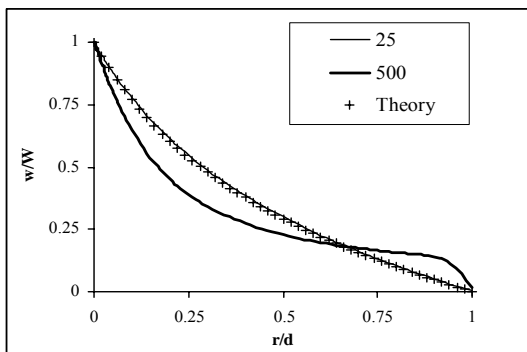


Fig.1 Tangential velocity profile at Re_D=25 and Re_D=500 compared with the theoretical equation 6.

The theoretical velocity profile can be derived from first principles as

$$\frac{w}{W_{max}} = \frac{\eta}{1 - \eta^2} \left(\frac{R_o}{r} - \frac{r}{R_o} \right) \tag{6}$$

where η is ratio of the inner to outer cylinder radius and R_o is the radius of the outer cylinder and r is the radial distance from the axis of the inner cylinder. Figure 1 shows the theoretical velocity profile also for the Couette flow case. Excellent agreement is found between the predicted and the theoretical velocity profiles. Typical radial velocity contours in the annular region are shown in Figure 2 along the radial plane at a Reynolds number, Re_D 96 and the radius ratio 0.30. The contours show that the Taylor vortices have already been formed at this Reynolds number. For a given radius ratio, the Taylor cells are formed beyond a critical Reynolds number [13]. It has been found that this critical value has been predicted well for the three radius ratios considered in the present study.

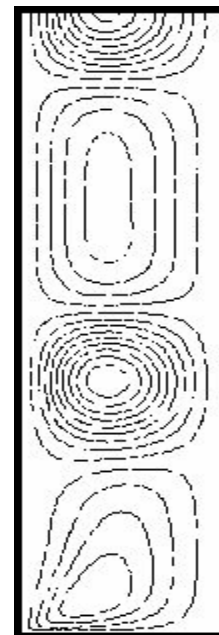


Fig.2 Radial velocity contours at Reynolds number Re_D of 96 for radius ratio of 0.30.

3.2 Effect of L/D_h ratio

Typically, a number of Taylor cells are set up if the cylinder height is long enough. The wall shear stress variation along the height is shown in Figure 3. This shows that except close to the bottom wall, a periodic shear stress variation, consistent with the Taylor cell pattern, is obtained on the inner cylinder surface. Thus, for a long enough height, a repeating pattern is obtained. However, if the cylinder height

is less, it is possible that the L/D_h ratio has an effect on the Taylor cell pattern. In order to investigate this, some calculations have been performed with the cylinder height increased by a factor of two to 0.24 m.

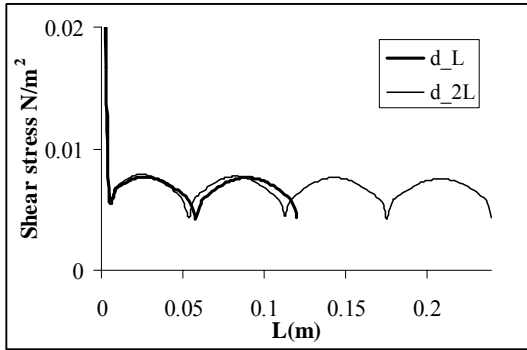


Fig.3 Wall shear stress variation along the height of the cylinder at $Re_D=760$.

The resulting axial shear stress variation is compared in Figure 3 for a Reynolds number Re_D of 760. It can be seen that the shear stress variation for the shorter cylinder case overlaps that for the longer cylinder case. Calculations with a wider gap show however that the predicted pattern may be affected if the gap width is increased by a factor of two while keeping the same height. These calculations show that the minimum height of the cylinder should be so as to allow a couple of Taylor cells to be resolved. Since the cell height is typically about the same as the gap width (see Figure 2), it can be concluded that the effect of liquid height would not be significant if $L/D_h > 2$.

3.3 Effect of radius ratio

The effect of radius ratio on the dimensionless velocity profiles for Couette regime and Taylor vortex regime is summarized in Figure 4 and Figure 5, respectively. Here the dimensionless tangential velocity is plotted in terms of dimensionless radial distance for three radius ratios, namely, 0.632, 0.462, 0.300 at a Reynolds number, Re_D of 50 which corresponds to before the onset of Taylor vortex and at a Reynolds number, Re_D of 760 which corresponds to after the onset.

From Figure 4, we note that, for small gap widths or high values of η , the radial velocity profile is linear. As η decreases, the velocity profile becomes non-linear, though monotonically decreasing. In the Taylor vortex regime condition also as shown in Figure 5 the radius ratio has a significant effect on the tangential velocity profile.

It is therefore to be expected that the radius ratio will have a parametric influence on the power number.

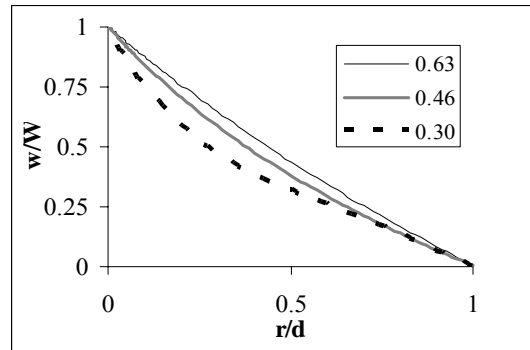


Fig.4 Tangential velocity profiles for three radius ratios in Couette flow region. $Re_D=50$.

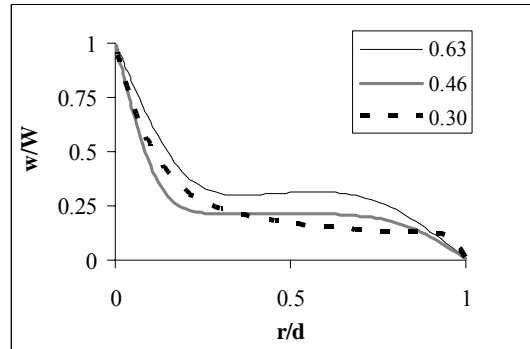


Fig.5 Tangential velocity profiles for three radius ratios in Taylor vortex region. $Re_D=760$.

3.4 Effect of Reynolds number

At very low Reynolds number, the flow is of Couette type and as the Reynolds number increases, Taylor vortex flow is set up. The variation of the power number with Reynolds number exhibits different characteristics in these two regimes as shown in Figure 6 and Figure 7. In the Couette flow, the power number (Po) varies as

$$Po \propto Re_{Dh}^{-1} \quad (7)$$

which is consistent with the experimental data of Sinevic et al. [1]. In the Taylor vortex flow regime, the power number varies as

$$Po \propto Re_{Dh}^{-n} \quad \text{where } n \sim 0.7 \quad (8)$$

which again is consistent with the data of Sinevic et al. [1]. The CFD simulations show that, in the range of radius ratios investigated, the variation is as given by equation (7). However, the exponent n in equation (8) for Taylor vortex conditions is found to be different for different radius ratios as illustrated

in Figure 8. This may be attributed to the short L/D_h employed in the present case (which is typical of solid dissolution applications). As seen from Figure 3, the application of zero velocity boundary condition on the bottom surface of the flow domain leads to a typical variation of the wall shear stress near the bottom wall. The wall shear stress, and hence the torque acting on the rotating cylinder, is thus not the same as that acting on an infinitely long cylinder in the same configuration. In the typical Taylor-Couette flow literature, long aspect ratios (large values of L/D_h) resulting from small annular gaps are employed and hence the asymmetric bottom boundary condition effect is not accounted for. This may be important in mass transfer applications where the cylinder heights are small and the annular gaps are large.

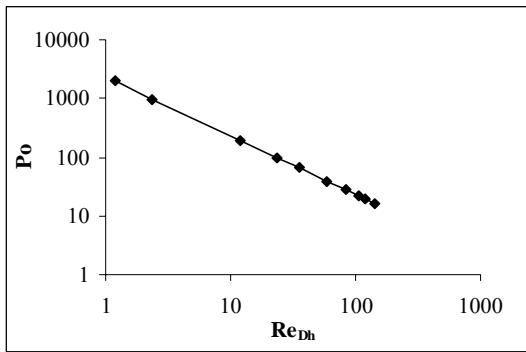


Fig.6 Power number variation with Reynolds number in the Couette flow regime for a radius ratio of 0.30.

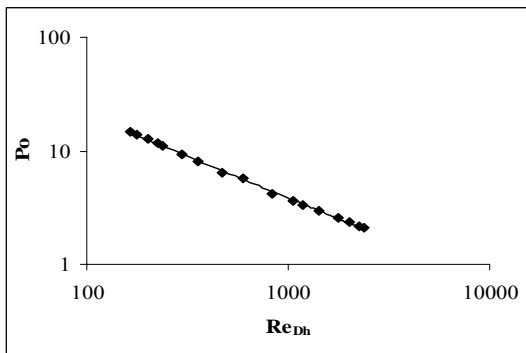


Fig.7 Power number variation with Reynolds number in the Taylor vortex flow regime for a radius ratio of 0.30.

3.5 Correlation for Power number

Using the numerical "data" obtained from the CFD simulations, the following correlations for the Power number have been developed which take account of

three parameters, namely, Reynolds number, radius ratio and the L/D_h ratio (Γ):

For the Couette flow regime,

$$Po = 310 Re_{Dh}^{-1} \eta^{-2.25} (1 - e^{-0.4\Gamma}) \quad (9)$$

For the Taylor vortex flow regime,

$$Po = 120 Re_{Dh}^{-0.7} \eta^{-1.75} (1 - e^{-0.4\Gamma}) \quad (10)$$

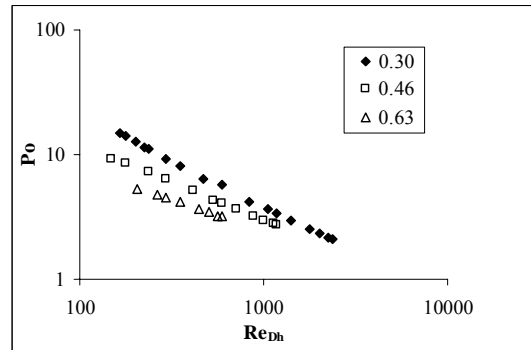


Fig.8 Power number variation with Reynolds number for three different radius ratios in Taylor vortex flow regime.

The transition between the Couette flow regime and the Taylor vortex flow regime is described in terms of the critical Taylor number given by DiPrima et al. [13]. Figure 9 shows comparison between the power number correlation (Eq. 10) and the experimental data of Sinevic et al. [1] for a radius ratio of 0.7, which shows very good agreement between the two.

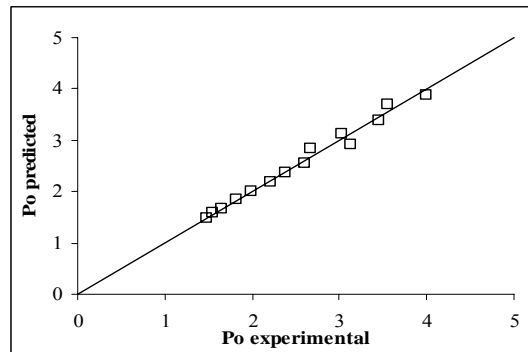


Fig.9 Comparison between Power number predicted (Equation 10) and experimental data of Sinevic et al [1] at radius ratio of 0.7 for Taylor vortex flow regime.

4 Conclusion

In the present paper, the flow field, and the power number have been predicted for an inner rotating cylinder in a stationary cylindrical vessel. The results show that the onset of Taylor vortices has a strong effect on the flow field. The power number (Po) varies as $Po \propto Re_{Dh}^{-1}$ in the laminar Couette region and $Po \propto Re_{Dh}^{-0.7}$ in the laminar Taylor vortex region for different radius ratios considered. Correlations are proposed for power number as a function of Reynolds numbers, radius ratio and the L/D_h ratio.

Acknowledgement: The calculations reported here have been done using the computational facilities of the CFD Centre, IIT-Madras, India.

Nomenclature:

A	area of the cylinder, m^2
d	gap width, m
D	cylinder diameter, m
D_h	hydraulic diameter, $2d$, m
i, o	inner and outer cylinder
L	cylinder height, m
P	power required
Po	Power number, $P/\rho N^3 D_i^5$
N	revolutions per second, rps
r	radial distance from the wall of the inner cylinder, m
R	cylinder radius, m
Re_{Dh}	Reynolds number based on hydraulic diameter, $\Omega R_i(2d) / \nu$
Re_D	Reynolds number based on inner cylinder diameter, $\Omega R_i(D_i) / \nu$
t	time, s
T	torque
u,	axial velocity, m/s
v	radial velocity, m/s
w	tangential velocity, m/s
W_{tip}	inner cylinder surface speed, $R_i * \Omega$, m/sec

Greek letters

Ω	angular velocity, rad/s
ρ	density, kg/m^3
ν	kinematic viscosity, m^2/s
η	radius ratio, R_i/R_o
τ_z	z-component shear stress, N/m^2
Γ	height-hydraulic diameter ratio, L/D_h

References:

[1]Sinevic. V, R. Kuboi and A.W. Nienow, Power numbers, Taylor numbers and Taylor vortices in

viscous Newtonian and Non-Newtonian fluids, *Chemical Engineering Science*, Vol.41, No.11, 1986, pp. 2915-2923.

- [2]Taylor. G.I, Stability of a Viscous Liquid Contained Between Two Rotating Cylinders, *Philos. Trans. Roy. Soc. London., A* Vol.289 1923, pp. 283.
- [3]Di Prima. R.C, H.L. Swinney, Instabilities and transition in flow between concentric rotating cylinders, in: H.L.Swinney, J.P. Gollub (Eds.), *Hydrodynamic Instabilities and the Transition to Turbulence*, Springer, Berlin, 1981, pp. 139-180.
- [4]Koschmieder. E.L, *Bénard Cells and Taylor Vortices*, Cambridge University Press, Cambridge, 1993.
- [5]Kataoka. K, Taylor vortices and instabilities in circular Couette flows. In *Encyclopedia of Fluid Mechanics*, Gulf Publications, Houston, Vol. 1, 1986, pp. 236-274.
- [6]Holman K.L, S.T. Ashar, Mass Transfer in Concentric Rotating Cylinders with Surface Chemical Reaction in the Presence of Taylor Vortexes, *Chem. Eng. Sci*, Vol.26, 1971, pp.1817-1831.
- [7]Baier. G, T.M. Grateful, M.D. Graham, E.N. Lightfoot, Prediction of Mass Transfer Rates in Spatially Periodic Flows, *Chem. Eng. Sci*, Vol.54, 1999, pp. 343-355.
- [8]Srinivasan. R, S.Jayanti, A.Kannan, Effect of Taylor Vortices on Mass Transfer from a Rotating Cylinder, accepted for publication in *AIChE.J*, 2005
- [9]Rhie. C..M, and W.L. Chow, Numerical Study of the Turbulent Flow Past an Airfoil with Trailing Edge Separation, *A.I.A.A. Journal*, Vol.21, No.11, 1983, pp 1527-1532.
- [10]Leonard. B.P, A stable and accurate modeling procedure based on quadratic upstream interpolation, *Comp. Methods. Appl. Mech. Eng*, Vol.19, 1979, pp 59-98
- [11]Hirsch. C, *Numerical computation of internal and external flows*, John Wiley & Sons, Inc., England, 1990.
- [12]Shekhar. S.M, S.Jayanti, CFD study of Power and Mixing time for Paddle mixing in Unbaffles vessels, *Trans IChem*, Vol.80, Part A, 2002, pp 482-498.
- [13]DiPrima. R.C, P.M. Eagles, B.S. Ng, The effect of radius ratio on the stability of Couette flow and Taylor vortex flow, *Phys. Fluids*. Vol.27, No.10, 1984, pp.2403-2411.